

Article

Development of Photocatalytic Coatings by Thermal Hydrolysis of TiCl_4 on Ceramic Roofing Tiles Made from Ferroalumina and Evaluation of De-Pollution Properties

Angeliki Christogerou ^{1,2,*}, Dimitra Koumpouri ³ and George N. Angelopoulos ^{1,2}

¹ Department of Chemical Engineering, University of Patras, Caratheodori 1, 26504 Patras, Greece; angel@upatras.gr

² INVALOR: Research Infrastructure for Waste Valorization and Sustainable Management, Caratheodory 1, University Campus, 26504 Patras, Greece

³ Institute of Nanoscience & Nanotechnology, National Center for Scientific Research Demokritos, Agia Paraskevi, 15342 Athens, Greece; d.koumpouri@inn.demokritos.gr

* Correspondence: angiechristo@upatras.gr; Tel.: +30-26-10-969-528

Received: 15 December 2019; Accepted: 28 January 2020; Published: 30 January 2020



Abstract: The development of new, environmental friendly building materials with photocatalytic properties remain still on the top of the investigations both for academy and industry. The main drive is the increasing air pollution and the greenhouse gas emissions that have negative effect on public health and buildings. Ceramic roofing tiles functionalized with TiO_2 can contribute on tackling these severe environmental problems by improving their properties. In this study, heavy clay ceramics manufactured from clay-body mixture and a Bayer process bauxite residue (ferroalumina) are used as substrates for the deposition of TiO_2 coatings in order to produce self-cleaning ceramic surfaces. The process is based on the thermal hydrolysis of TiCl_4 which takes place in a CVD reactor under atmospheric conditions. All coated samples were annealed at 600 °C and characterized in means of XRD, SEM/EDS and degradation ability of an organic pollutant. The formation of titania mixed phases (rutile and perovskite) shows positive results regarding the photocatalytic activity of the samples. The ones containing ferroalumina decomposed 100% the indigo carmine solution after 4 h, in comparison with the reference one which presented lower efficiency. Finally, this paper addresses technical feasible solutions for the production of photocatalytic active ceramics within the concept of circular economy and environmental sustainability.

Keywords: clay roofing tiles; industrial by-product; ferroalumina; chemical vapor deposition; hydrolysis of TiCl_4 ; TiO_2 coatings; dye degradation; circular economy; antipollution

1. Introduction

The production of “smart” building materials and coatings designed on the basis of TiO_2 has gained special attention in the last decade. In particular, the development of new technologies with regards to titania is targeted on self-cleaning surfaces and environmental applications. In this aspect, traditional ceramics such as roofing tiles are considered as good candidates for novel applications by enhancing their conventional properties into new ones with photocatalytic features [1,2]. This can be achieved through the development of functional coatings that consist of metal oxides such as titanium dioxide (TiO_2). The later oxide has been proven to be an ideal photocatalyst in many fields of everyday applications like cosmetics, food, paints, ceramic glazes, textiles, and even in medicine [3,4] due to its excellent properties.

One of these properties that attract great interest is the ability of TiO_2 to participate in red-ox reactions which are activated under UV irradiation [5–7] leading to substantial reduction of airborne pollutants such as volatile organic compounds and nitrogen oxides (NO_x gases). The fundamental mechanism that takes place in heterogeneous photocatalysis with titania after irradiated by light ($h\nu \geq E_g = 3.2 \text{ eV}$) is the production of a reactive electron (e^-)/hole (h^+) pair ($\text{TiO}_2 + h\nu \rightarrow \text{TiO}_2 + h^+ + e^-$). The photogenerated electrons (e^-) can react with oxygen molecules (O_2) from the atmosphere to form superoxide radicals ($\cdot\text{O}_2^-$). Accordingly, the positively charged surface of TiO_2 (h^+) can not only directly oxidize organic compounds due to its strong oxidizing ability, but also react with water molecules (moisture from the air) to form hydroxyl radical ($\cdot\text{OH}$) [8]. These active species can then decompose adsorbed organic pollutants to CO_2 and water [2,9].

Another positive aspect of the heterogeneous photocatalysis with TiO_2 are the conditions under which the reaction can take place, i.e., low level of UV radiation, room temperature and atmospheric pressure. Moreover, no chemical additives are necessary and the possible intermediates of the reactions are not dangerous or at least less dangerous than the original pollutant, even every recalcitrant and persistent pollutants can be degraded [3,10]. Thus, taking into account that UV radiation is present in daylight, and even on cloudy days, makes the TiO_2 coatings very attractive to outdoor building materials. In addition, the aesthetic result of coated surfaces remains unaffected in case of nano-crystalline thin films that are transparent and colorless [11]. However, the photocatalytic activity of TiO_2 is affected by different factors such as production techniques and conditions of preparation, surface properties and TiO_2 phases (crystallinity, crystallite size, and symmetry).

Regarding the production of titania nanoparticles and the related deposition techniques numerous scientific reports are found in the open literature. For example, it is stated in [12] that the nanocrystallinity of titania is strictly connected with the enhancing of the photocatalytic activity, due to the fact that it favors the diffusion on the surface of free electron and holes and limits their recombination through charge carrier trapping. Additionally, it has been observed that anatase (A) or mixture phases (anatase/rutile) present higher photoactivity than the pure crystalline phases of TiO_2 like rutile (R) and brookite [1,13,14]. Zeatoun et al. [15] produced submicron TiO_2 smoke by hydrolysis of TiCl_4 at reactor temperatures between 210°C and 817°C . Higher reactor temperatures ($405\text{--}817^\circ\text{C}$) favor the formation of anatase, while amorphous powders resulted on lower reactor temperatures. Watanabe et al. [16] report that the activity of the photocatalytic fabricated tiles increases with the firing temperature up to 700°C and presents the opposite effect when sintered at higher temperatures due to the transformation of anatase to rutile. In addition, TiO_2 films loaded with metal additives (CuO) remarkably enhance their photocatalytic activity after firing at 900°C . Sun et al. [17] prepared TiO_2 films on glass by CVD at atmospheric pressure using TiCl_4 as a precursor. They found that the ideal deposition is obtained when the spacing between nozzle and glass is about 3 mm. The deposition rate was found to increase with the substrate temperature. Anatase was detected as major crystalline phase and the degeneration efficiency of methyl orange increases with increase of deposition temperature. Song et al. [18] studied the deposition TiO_2 on muscovite flakes doped with different metal ions using chemical liquid deposition method. Some metal ions (Mn^{2+} , Sn^{4+} , Fe^{3+} and Zn^{2+}) promote the A-R transformation whilst others (Al^{3+} , Cu^{2+} , Co^{2+}) inhibit it. Calcination temperature influences as well the A-R transformation which starts at 800°C and is completed at 1000°C . Ding et al. [19] studied the synthesis of anatase TiO_2 supported on three different porous solids by CVD and evaluated their photocatalytic activity. Silica gel was found to be the most efficient support in terms of both anatase formation and photocatalytic reaction.

In recent years, studies on new types of semiconductor catalysts have gained also remarkable interest as for perovskite compounds. Perovskite (CaTiO_3) with the general formula ABO_3 is frequently encountered structure in inorganic chemistry and can accommodate most of the metallic ions in the periodic table with a significant number of different anions. According to those studies perovskite can be used as a catalyst [6,20,21].

The evaluation of photocatalytic coatings involves a number of analyses; the most frequent used are SEM (microstructure, grain size and shape of particles), XRD (crystalline phases) and degradation of dyes giving valuable information about the materials performance. However, it is reported [22] that the evaluation of self-cleaning properties and photocatalytic degradation of pigments, concretes or non-transparent materials are limited in means of scientific literature and standard methods, compared to coated glasses which are commercially available. Nevertheless, the self-cleaning ability of opaque and rough surfaces is measured by reflectance spectroscopy as defined by the European standard EN 16845-1:2017 [23].

Despite the large number of studies available in the open literature concerning the production of TiO₂ coatings on different supports, only few are focused on the production of photocatalytic heavy clay materials. Tobaldi et al. [3] investigated the addition of TiO₂ powders in a clay body mix suitable for the production of heavy clay products and examined the factors which influence their photocatalytic activity. Moreover, Ducman et al. [2] studied the formation of photocatalytic coatings on ceramics building products (tiles, glass and roofing tiles) by spraying of a TiO₂ isopropanol suspension. Another scientific work related to TiO₂ functional tiles was performed by Vaiano et al. [24] who examined the influence of the substrates porosity on the photocatalytic activity of coated ceramic tiles. However, no work was found, up to now, in the literature regarding the application of Chemical Vapour Deposition (CVD) for the production of coated heavy clay ceramics.

In the current study, the development of photocatalytic active TiO₂ spots on ceramic roofing tiles were studied using CVD as a coating method. For this purpose, feasibility tests were conducted, in laboratory scale, by depositing TiCl₄ as a precursor solution on ceramic samples. The photocatalytic properties of the coated and annealed surfaces were successfully examined by XRD, SEM/EDS and decolorization ability of an indigo carmine solution. Finally, the technological outcomes of this work may be used as a basis for large-scale investigations, with the future perspective of an industrial scale application.

2. Materials and Methods

2.1. Ceramic Substrates

The ceramic substrates used for the deposition of TiO₂ are shown in Figure 1. They consist mainly of a calcareous rich Greek clay mixture (W) and ferroalumina (FA) in different percentages. Ferroalumina is an industrial by-product that derives from the dewatering of red mud, a bauxite residue of the Bayer's process [25]. For the current investigation cylindrical samples (d = 5 cm, h = 1 cm) were cut off by a diamond hollow drill from rectangular ceramic samples fired at 1000 °C and named according to the included percentage of FA such as S0 (0 wt%), S10 (10 wt%), S20 (20 wt%), and S50 (50 wt%). The experimental procedure for their manufacture is described elsewhere [26].

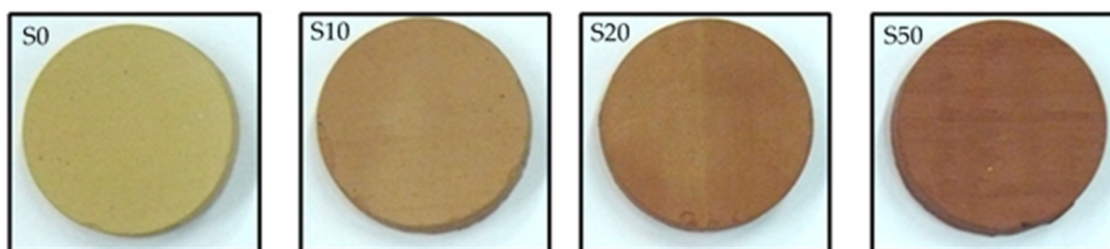


Figure 1. Fired (1000 °C) ceramic substrates with different amounts of ferroalumina. S0 (0 wt% FA), S10 (10 wt% FA), S20 (20 wt% FA).

2.2. Characterization Techniques

The chemical composition of the raw materials was determined by Atomic Absorption Spectrometer (AAAnalyst 200, Perkin Elmer, Shelton, CT, USA). The mineralogical characterization

of the coated surfaces was carried out by X-ray diffraction analysis (Siemens Diffraktometer D5000, Karlsruhe, Germany) in the $10\text{--}70^\circ$, 2θ range with a step size of 0.01° and a speed of $1^\circ/\text{min}$. For the XRD measurements, Cu K α radiation at 40 kV and 30 mA was used. The crystalline phases identified using the DIFFRACplus EVA12® software (Bruker-AXS, Billerica, MA, USA) based on the ICDD powder diffraction file of PDF-2 2006. The mineralogical phases were quantified with the Rietveld-based routine using the TOPAS® software (Diffrac^{Plus} Professional, Version 4.2, Bruker-AXS, Karlsruhe, Germany). The morphology and size of the titania particles were analyzed by SEM/EDS (JSM-6300, Jeol, Tokyo, Japan) equipped with an X-ray energy dispersive spectrometer on gold coated surfaces.

2.3. CVD Apparatus and Procedures

For the CVD process, a small experimental set-up was constructed and is depicted in Figure 2. TiCl_4 (99.9% purity, Acros Organics™, New Jersey, NJ, USA) was used as a precursor solution to form TiO_2 spots on the ceramics' surface. The liquid TiCl_4 was placed in a spherical glass vessel within a nitrogen filled glove box in order to prevent vigorous reaction with moisture in the air. During the experiment, the glass vessel was heated by an electric heating mantel and the external temperature of the flask was measured using a K type thermocouple connected to a PID temperature controller. Nitrogen (99.9%) was used as a carrier gas to transport the vaporized precursor to the reactor chamber (cylindrical quartz tube) with a flow rate of $0.125\text{ cm}^3/\text{s}$. This rate results in a sufficient inflow of TiCl_4 in order to achieve the formation of small size (sub-micron scale) TiO_2 particles on the surface of the ceramics providing high reactive surface as well as the desirable adhesion with the substrate. Additionally, the used flow rate leads to the creation of an invisible TiO_2 coating which does not affect the natural appearance of the ceramics. It was observed from our preliminary tests that higher inflow rates of the precursor led to the formation of a liquid gel which upon drying turned to a greenish powder attributed to chlorine contamination. Consequently, the formed coating was fragile and presented poor adhesion with the substrate. Similar behaviour is reported also elsewhere [19]. Wet scrubbing was employed at the outlet of the reactor using a caustic trap (Na_2CO_3 solution) for the removal of residual TiCl_4 and other vapor by-products.

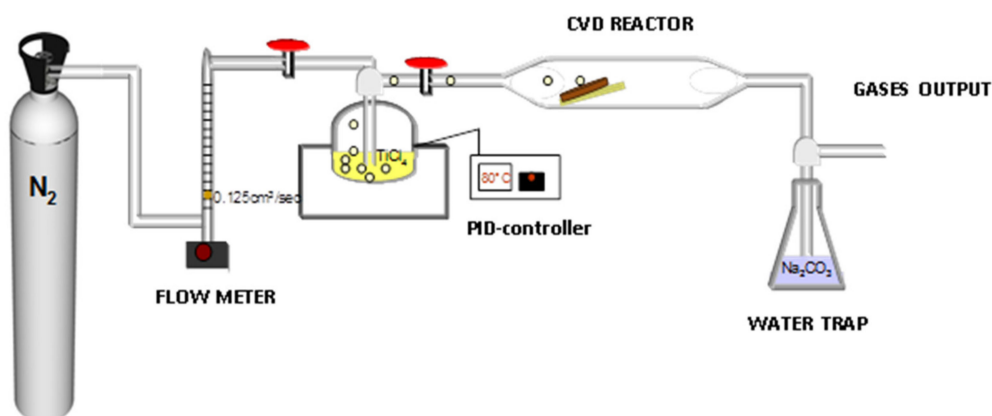


Figure 2. Schematic representation of the experimental CVD setup.

The ceramic samples were sprayed with a solution containing Cu^{2+} ions and then placed in a suitable support at an angle of 20° , which was 15 cm approximately far from the nozzle. Metal ions are known to enhance both the crystallinity of TiO_2 and the photoactivity of the final coating [16]. The temperature of the liquid TiCl_4 was maintained at $60\text{--}80^\circ\text{C}$ during the whole process. The experimental procedure was carried out under atmospheric pressure and the deposition lasted for one hour. After the CVD process, the coated samples were annealed up to 600°C in a laboratory muffle furnace for 1 hour and a heating rate of $20^\circ\text{C}/\text{min}$.

2.4. Photocatalytic Degradation Experiments

The photocatalytic activity of the coated samples was evaluated by the degradation ability of an Indigo Carmine (IC) solution under UV irradiation. The organic dye was purchased from ACROS Organics™ (New Jersey, NJ, USA). A stock solution (100 ppm) was prepared by dissolving and diluting 50 mg of Indigo Carmine to 500 mL in deionized water (Millipore, Direct Q-3, Molsheim, France). For the experiments, a cylindrical glass vessel was filled with 500 mL of the test solution (1 ppm). To ensure continuous flow of the liquid and removal of the surface reactants magnetically stirring was employed during the whole process. The coated substrate was placed in a suitable base; 10 mm under the water's surface in order to be near the light source. UV irradiation was provided by two parallel blacklight blue lamps (6 W, Sen-lite, F6T5/BLB) with a wavelength of $\lambda = 365$ nm, which were placed horizontally above the sample. The light intensity reaching the samples surface was measured at 10 W/m². The tests were carried out under ambient conditions at room temperature.

Prior to all photocatalytic experiments, the IC solution was magnetically stirred for 30 min in dark in order to achieve adsorption equilibrium [6]. During irradiation, sampling from the reacting system took place every one hour. The obtained liquid was filtered through a 0.45 µm Porafil filter disk and analyzed by absorbance spectroscopy (Milton Roy, Spectronic® Genesys™ 5, Rochester, NY, USA) at a wavelength of 610 nm using quartz cuvettes. The photocatalytic performance of the coated ceramics was studied according to the decolorization of indigo carmine using the following equation:

$$\text{Photocatalytic efficiency} = \eta \% = \frac{A_0 - A_s}{A_0} \times 100 \quad (1)$$

where A_0 is the initial absorption of the dye and A_s the absorption of the dye after a certain UV irradiation time.

3. Results and Discussion

3.1. Physico-Chemical Properties of Ceramic Substrates

The chemical composition of the raw materials used for the production of the ceramic samples is shown in Table 1. The clay mixture (W) presents a typical composition of Ca-rich clay material suitable for the production of white-body ceramics. Ferroalumina (FA) is rich in iron oxide (44.34%) and titanium oxide (5.12%) which is expected to contribute on the photocatalytic efficiency of the coated samples.

Table 1. Chemical analysis of raw materials (in wt%). W: clay mixture and FA: ferroalumina.

| | SiO ₂ | Al ₂ O ₃ | CaO | Fe ₂ O ₃ | MgO | K ₂ O | Na ₂ O | TiO ₂ | L.O.I. |
|----|------------------|--------------------------------|-------|--------------------------------|------|------------------|-------------------|------------------|--------|
| W | 48.29 | 13.61 | 12.72 | 5.30 | 3.11 | 2.49 | 0.59 | n.d. | 13.64 |
| FA | 7.79 | 17.04 | 11.64 | 44.34 | 0.57 | 0.07 | 3.17 | 5.12 | 9.77 |

n.d.: not determined.

The mineralogical compositions of the fired ceramic surfaces are presented in Table 2. For the reference samples (S0) the identified phases are quartz (SiO₂), albite (NaAlSi₃O₈), diopside (CaMgAl₂Si₂O₆), and calcite (CaCO₃). Hematite (Fe₂O₃) was additionally formed in case of S10, S20, and S50 which increases according to the ferroalumina content in the mixes.

Table 2. Quantitative (wt%) mineralogical composition of the uncoated ceramic samples.

| | Quartz | Albite | Calcite | Diopside | Hematite |
|------------|--------|--------|---------|----------|----------|
| S0 | 27.9 | 17.9 | 14.1 | 40.1 | n.d. |
| S10 | 22.7 | 14.4 | 11.3 | 45.4 | 6.2 |
| S20 | 21.3 | 7.9 | 10.9 | 46.4 | 13.5 |
| S50 | 9.6 | n.d. | 25.5 | 20.6 | 44.2 |

n.d.: not determined.

3.2. Crystalline Phases and Morphology of Coated Surfaces

XRD patterns of the coated and annealed (600 °C) surfaces are shown in Figure 3, whereas the results of the quantitative analysis are presented in Table 3. In all compositions, new formed TiO₂ phases were identified coexisting with the mineralogical phases of the non-coated ceramics (Table 2). The reference sample (S0) showed the presence of perovskite at 5.2 wt%. For the samples S10 and S20 the formation of mixed-TiO₂ phases is observed, consisting of rutile (~2.1 wt%) and perovskite (~5.2 wt%). In case of S50, only rutile was detected at 5.7 wt%. The formation of perovskite in the case of S0, S10, and S20 ceramics could be attributed to the presence of albite which act as Ca²⁺ source and reacts with the deposited TiO₂ during the CVD process. On the other hand, the absence of albite in sample S50 leads only to the deposition of TiO₂, which after the annealing crystallizes in rutile phase.

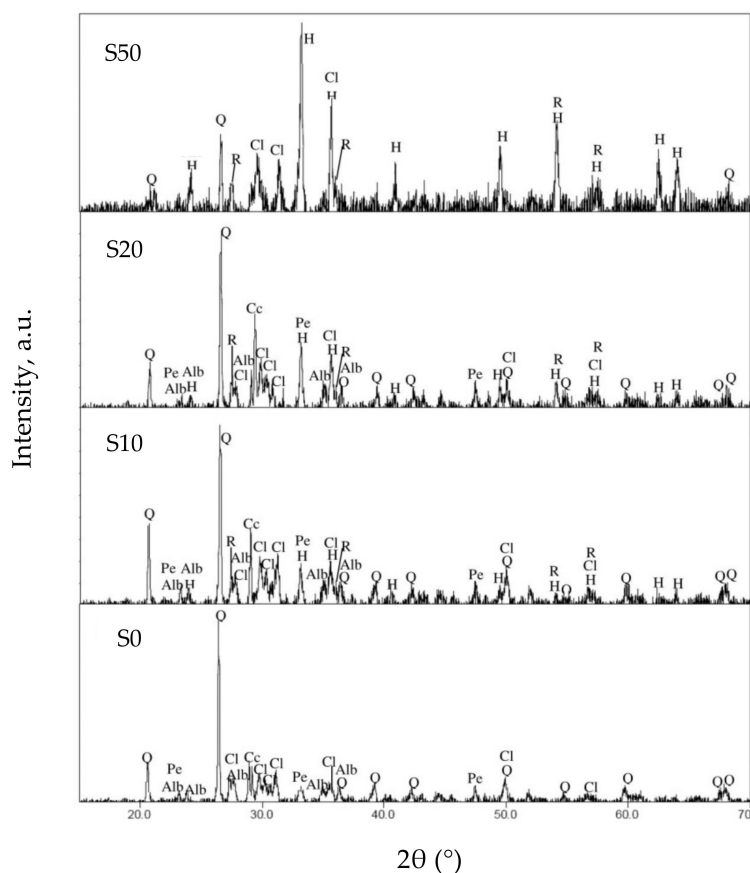
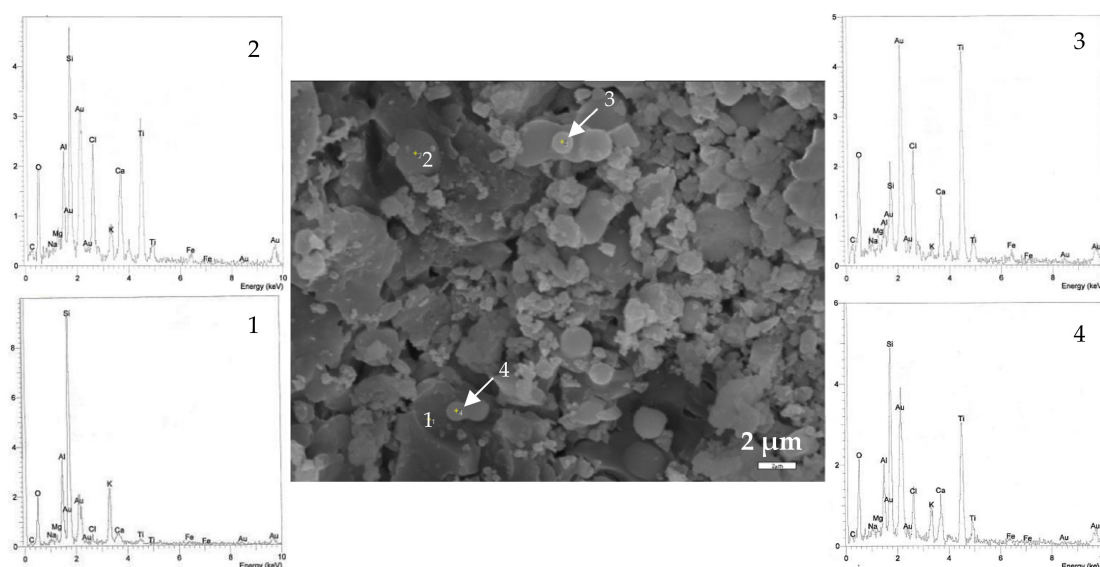
**Figure 3.** XRD patterns of coated surfaces, after annealing at 600 °C for 1 h. Abbreviations— Q: quartz, Alb: albite, Cl: clinopyroxene (aluminium diopside), Cc: calcite, H: hematite, Pe: perovskite, R: rutile.

Table 3. Quantitative (wt%) mineralogical composition of coated ceramics.

| | Quartz | Albite | Calcite | Diopside | Hematite | Rutile | Perovskite |
|------------|--------|--------|---------|----------|----------|--------|------------|
| S0 | 22.4 | 18.7 | 15.1 | 38.5 | n.d. | n.d. | 5.2 |
| S10 | 19.3 | 15.1 | 14.1 | 42.1 | 2.2 | 2.2 | 5.1 |
| S20 | 19.0 | 8.7 | 13.1 | 43.6 | 8.2 | 2.1 | 5.3 |
| S50 | 9.0 | n.d. | 26.6 | 19.8 | 38.9 | 5.7 | n.d. |

n.d.: not determined

SEM images of coated and annealed (600 °C) ceramic surfaces are presented in Figures 4–6. The developed titania coatings on their surfaces is confirmed by EDS analyses revealing that spherical particles are rich in Ti. However, the biggest challenge is to distinguish the different morphologies of TiO₂ phases, as they were detected in XRD analysis (e.g., rutile and perovskite), both due their small crystal size and the strong interference of the ceramics microstructure (e.g., porosity and microroughness).

**Figure 4.** SEM image (4000×) and energy spectrum analysis (1–4) of the coated reference sample S0, after annealing at 600 °C for 1 h.

The reference sample (S0), Figure 4, exhibits these spherical particles which appear to have been formed sporadically on the ceramics surface with a size up to 2 µm (Figure 4, points 3 and 4). However, it is not unlikely to detect Ti also on other micro-regions, in form of perovskite (CaO·TiO₂) as shown from the relative energy graph (Figure 4, (2)); consistent with the XRD results (Table 3). The ratio of Ca and Ti according to the atomic analysis is close to 1:1.

In case of S10, Figure 5, well-formed spherical particles of titania (Figure 5, (1)) have been formed next to flake-like crystals which are rich in Cu, Figure 5, (3), as a result of the doping procedure on the ceramics surfaces. The microstructure presents diversities compared to S0, as small agglomerations are observed among the typical ceramic microstructure closely related to the contained ferroalumina in the raw mix.

The sample S20, Figure 6, shows a different surface morphology compared to the other samples representing a stronger tendency to particle agglomeration attributed to the increased amount of ferroalumina and its related fine particle size. Spherically-formed particles are larger in size, varying from 4 to 8 µm which is typical for low reactor temperatures [15]. EDS analysis confirms the formation of perovskite (Ca:Ti = 1:1).

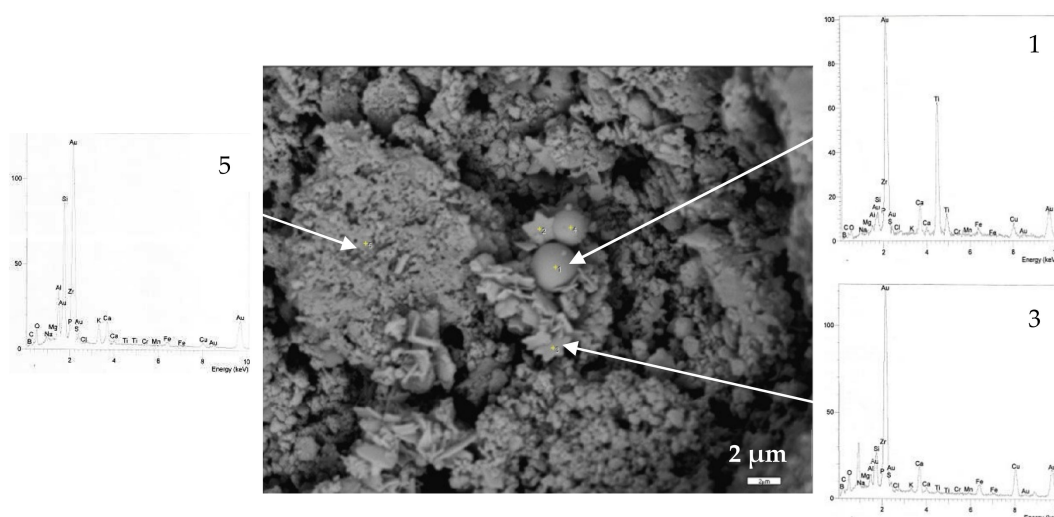


Figure 5. SEM image (3500×) and energy spectrum analysis of coated S10, after annealing at 600 °C for 1 h.

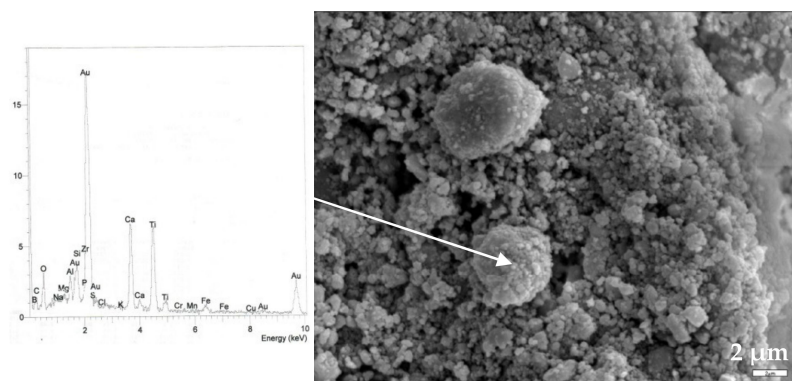


Figure 6. SEM image (4000×) and energy graph of coated surface S20, after annealing at 600 °C for 1 h.

3.3. TiO_2 Synthesis

In a low-pressure CVD process the synthesis of TiO_2 can be represented by the following reaction:



The presence of water is important for the hydrolysis of TiCl_4 and the formation of the TiO_2 coating. Thus, the surface of the ceramic samples must have the appropriate humidity in order to achieve the desired coating. Moreover, HCl dissolves calcium compounds to CaCl_2 which is anticipated to react with TiO_2 in order to form perovskite (CaTiO_3) that is in agreement with the obtained XRD results (Figure 3).

3.4. Photocatalytic Degradation of Indigo Carmine

3.4.1. Preliminary Tests

Preliminary experiments were carried out on the decolorization of indigo carmine solution in order to exclude any possible photolysis due to other parameters apart from the TiO_2 catalyst. Tests were conducted using a solution of 1 ppm indigo carmine (a) in the absence of any ceramic sample, but under UV irradiation and (b) in the presence of uncoated samples and UV irradiation. Case (a) was performed to see if the dye solution undergoes self-decomposition with UV light and case (b) to ensure that the porosity of the ceramics does not affect the concentration of the dye due to adsorption.

The results showed no decolorization of the dye in case of (a). This means that the direct photolysis of IC solution under UV irradiation is excluded, in agreement with [27]. However, in case (b) the samples showed a small decolorization rate, Figure 7, varying from 5.3–10.5%, with the highest value corresponding to the samples S10 and S20; and the lowest to S0. Taking into account the technological properties of the ceramic samples, the water absorption capacity after 24h was found approximately 11%, while the apparent porosity was calculated [26] at 34.7% for S0 and S10, and 39.1% and 41.3% for S20 and S50, respectively. From the obtained results, it can be concluded that the highly porous nature of the samples does not directly influence the decoloring of the dye solution.

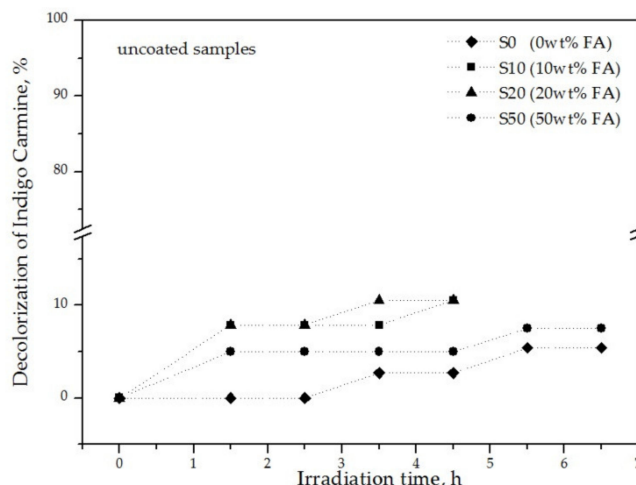


Figure 7. Decolorization ability of uncoated samples as a function of irradiation time.

3.4.2. Photocatalytic Activity of Coated Ceramics

The photocatalytic efficiency of the TiO_2 coated ceramic samples was examined under UV irradiation and the results are depicted in Figure 8. All coated samples were able to decolorize the dye but at different times and rates. In particular, the best photocatalytic activity was obtained for the samples S10 and S20 as they decomposed the dye 100% after four hours under UV exposure. S50 presented also 100% decomposition of IC solution but at six hours of irradiation. On the contrary, the reference sample S0 showed a significant lower degradation ability of about 29% after six hours of exposure to UV. Comparing the results obtained, it can be concluded that the presence of rutile combined with perovskite (S10 and S20) has the highest photocatalytic activity. Rutile's activity is adversely affected by the absence of perovskite (S50) only in terms of rate.

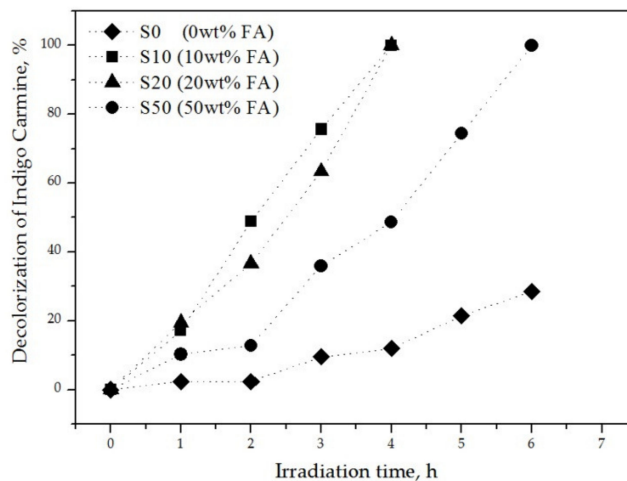


Figure 8. Decolorization (%) of IC solution as a function of irradiation time (h) for all coated samples.

4. Conclusions

The development of photocatalytic coatings on ceramic substrates with the method of CVD and hydrolysis of TiCl_4 was successful since promising results were obtained considering the surface characteristics (i.e., the formation of spherical titania spots) and the photodegradation of an organic pollutant. All coated samples presented photocatalytic activity, but at different rates and times. The addition of the industrial by-product ferroalumina as raw material in the clay-body mix seems to favour the degradation ability of the ceramics as the decomposition rate of Indigo Carmine solution reaches 100%. In particular, the most effective ones are the S10 and S20 which decompose at four hours, whereas S50 decomposes at six hours. At the same time, like the latter one, the reference sample was able to decompose only 28% of the dye solution. The correlations between the ferroalumina content in the ceramic samples and the photocatalytic performance is clearly related to the formation of rutile and/or perovskite, the combination of which exhibits the best photocatalytic activity (S10 and S20).

Author Contributions: Conceptualization, A.C. and G.N.A.; methodology, A.C. and D.K.; investigation, A.C. and D.K.; writing—original draft preparation, A.C.; writing—review and editing, A.C. and D.K.; project administration, A.C. All authors have read and agreed to the published version of the manuscript.

Funding: The authors acknowledge support of this work by the project “INVALOR: Research Infrastructure for Waste Valorization and Sustainable Management” (MIS 5002495) which is implemented under the Action “Reinforcement of the Research and Innovation Infrastructure”, funded by the Operational Programme “Competitiveness, Entrepreneurship and Innovation” (NSRF 2014–2020) and co-financed by Greece and the European Union (European Regional Development Fund).

Acknowledgments: The authors would like to thank Dr. Andreas Seferlis of the Laboratory of Electron Microscopy and Microanalysis (L.E.M.M.) of the University of Patras.

Conflicts of Interest: The authors declare no conflict of interest.

References

- Da Silva, A.L.; Dondi, M.; Raimondo, M.; Hotza, D. Photocatalytic ceramic tiles: Challenges and technological solutions. *J. Eur. Ceram. Soc.* **2018**, *38*, 1002–1017. [\[CrossRef\]](#)
- Ducman, V.; Petrovič, V.; Škapin, S.D. Photo-catalytic efficiency of laboratory made and commercially available ceramic building products. *Ceram. Int.* **2013**, *39*, 2981–2987. [\[CrossRef\]](#)
- Tobaldi, D.M.; Tucci, A.; Roda, G.C.; Baldi, G.; Esposito, L. Photocatalytic activity for exposed building materials. *J. Eur. Ceram. Soc.* **2008**, *28*, 2645–2652. [\[CrossRef\]](#)
- Munafò, P.; Goffredo, G.B.; Quagliarini, E. TiO_2 -based nanocoatings for preserving architectural stone surfaces: An overview. *Constr. Build. Mater.* **2015**, *84*, 201–218. [\[CrossRef\]](#)
- Balasubramanian, G.; Dionysiou, D.; Suidan, M.; Baudin, I.; Laine, J. Evaluating the activities of immobilized TiO_2 powder films for the photocatalytic degradation of organic contaminants in water. *Appl. Catal. B: Environ.* **2004**, *47*, 73–84. [\[CrossRef\]](#)
- Fujishima, A.; Rao, T.N.; Tryk, D.A. Titanium dioxide photocatalysis. *J. Photochem. Photobiol. C Photochem. Rev.* **2000**, *1*, 1–21. [\[CrossRef\]](#)
- Hashimoto, K.; Irie, H.; Fujishima, A. TiO_2 Photocatalysis: A Historical Overview and Future Prospects. *Jpn. J. Appl. Phys.* **2005**, *44*, 8269–8285. [\[CrossRef\]](#)
- Zhang, X.; Wang, J.; Dong, X.-X.; Lv, Y.-K. Functionalized metal-organic frameworks for photocatalytic degradation of organic pollutants in environment. *Chemosphere* **2020**, *242*, 125144. [\[CrossRef\]](#)
- Arsac, F.; Bianchi, D.; Chovelon, J.; Conchon, P.; Ferronato, C.; Lair, A.; Sleiman, M. Photocatalytic degradation of organic pollutants in water and in air. An analytical approach. *Mater. Sci. Eng. C* **2008**, *28*, 722–725. [\[CrossRef\]](#)
- Herrmann, J.-M.; Duchamp, C.; Karkmaz, M.; Hoai, B.T.; Lachheb, H.; Puzenat, E.; Guillard, C. Environmental green chemistry as defined by photocatalysis. *J. Hazard. Mater.* **2007**, *146*, 624–629. [\[CrossRef\]](#)
- Moreno, A. Ceramic tiles: above and beyond traditional applications. *Bol. Soc. Esp. Ceram. V.* **2006**, *45*, 59–64. [\[CrossRef\]](#)
- Yang, H.; Zhang, K.; Shi, R.; Tang, A. Sol-Gel Synthesis and Photocatalytic Activity of $\text{CeO}_2/\text{TiO}_2$ Nanocomposites. *J. Am. Ceram. Soc.* **2007**, *90*, 1370–1374. [\[CrossRef\]](#)

13. Chen, Y.; Stathatos, E.; Dionysiou, D.D. Microstructure characterization and photocatalytic activity of mesoporous TiO₂ films with ultrafine anatase nanocrystallites. *Surf. Coatings Technol.* **2008**, *202*, 1944–1950. [CrossRef]
14. Li, G.; Ciston, S.; Saponjic, Z.V.; Chen, L.; Dimitrijevic, N.M.; Rajh, T.; Gray, K.A. Synthesizing mixed-phase TiO₂ nanocomposites using a hydrothermal method for photo-oxidation and photoreduction applications. *J. Catal.* **2008**, *253*, 105–110. [CrossRef]
15. Zeatoun, L.; Feke, D. Characterization of TiO₂ Smoke Prepared Using Gas-Phase Hydrolysis of TiCl₄. *Part. Part. Syst. Charact.* **2006**, *22*, 276–281. [CrossRef]
16. Watanabe, T.; Kojima, E.; Norimoto, K.; Saeki, Y. Fabrication of TiO₂ photocatalytic tile and its practical applications. *Fourth Euro-Ceramics 11 Floor Wall Tiles* **1995**, 175–180.
17. Sun, H.; Wang, C.; Pang, S.; Li, X.; Tao, Y.; Tang, H.; Liu, M. Photocatalytic TiO₂ films prepared by chemical vapor deposition at atmosphere pressure. *J. Non-Crystalline Solids* **2008**, *354*, 1440–1443. [CrossRef]
18. Song, G.; Liang, J.; Liu, F.; Peng, T.; Rao, G. Preparation and phase transformation of anatase–rutile crystals in metal doped TiO₂/muscovite nanocomposites. *Thin Solid Films* **2005**, *491*, 110–116. [CrossRef]
19. Ding, Z.; Hu, X.; Yue, P.L.; Lu, G.Q.; Greenfield, P.F. Synthesis of anatase TiO₂ supported on porous solids by chemical vapor deposition. *Catal. Today* **2001**, *68*, 173–182. [CrossRef]
20. Kim, J.; Hwang, D.W.; Kim, H.G.; Bae, S.W.; Lee, J.S.; Li, W.; Oh, S.H. Highly Efficient Overall Water Splitting Through Optimization of Preparation and Operation Conditions of Layered Perovskite Photocatalysts. *Top. Catal.* **2005**, *35*, 295–303. [CrossRef]
21. Yang, Y.; Sun, Y.; Jiang, Y. Structure and photocatalytic property of perovskite and perovskite-related compounds. *Mater. Chem. Phys.* **2006**, *96*, 234–239. [CrossRef]
22. Minella, M.; Minero, C. Quantification of the Photocatalytic Self-Cleaning Ability of Non-Transparent Materials. *Materials* **2019**, *12*, 508. [CrossRef] [PubMed]
23. CEN European Committee for Standardization. *EN 16845-1:2017 Photocatalysis. Anti-Soiling Chemical Activity Using Adsorbed Organics under Solid/Solid Conditions. Part1: Dyes on Porous Surfaces*; CEN European Committee for Standardization: Brussels, Belgium, 2017.
24. Vaiano, V.; Sarno, G.; Sannino, D.; Ciambelli, P. Photocatalytic properties of TiO₂-functionalized tiles: influence of ceramic substrate. *Res. Chem. Intermed.* **2015**, *41*, 7995–8007. [CrossRef]
25. Red Mud Project - Site dedicated on the valorisation and best practices on bauxite residue. Available online: <http://redmud.org/> (accessed on 15 September 2019).
26. Pontikes, Y.; Nikolopoulos, P.; Angelopoulos, G. Thermal behaviour of clay mixtures with bauxite residue for the production of heavy-clay ceramics. *J. Eur. Ceram. Soc.* **2007**, *27*, 1645–1649. [CrossRef]
27. Vautier, M.; Guillard, C.; Herrmann, J.-M. Photocatalytic Degradation of Dyes in Water: Case Study of Indigo and of Indigo Carmine. *J. Catal.* **2001**, *201*, 46–59. [CrossRef]

